

# Static and Dynamic Loading Test on Base Foundation in a Reinforced Concrete School Building



**T. Kabeyasawa**

*National Institute for Land and Infrastructure Management, Japan*

**T. Kabeyasawa, & Y. Hosokawa**

*Earthquake Research Institute, The University of Tokyo, Japan*

**Y. Kim**

*Yonsei University, Korea*

## SUMMARY:

Dynamic and static loading tests were carried out on an existing building, which was a three-story reinforced concrete school with spread foundation to evaluate the lateral stiffness of spread foundations. The impact load was applied at the base foundation using the steel mass pendulum. The static loading test was also carried out from the other side at the foundation level. The non-linear behavior was observed as a hysteretic shape, although the maximum response displacements by the impact loading were not so large well in inelastic region. The maximum shear coefficient attained up to 2.1 during the pushover static test. The theoretical elastic stiffness of the spread foundation was evaluated, and approximated an elastic stiffness from the impact load test. The static friction test has been also carried out in the laboratory to evaluate the bonding or interlocking strength on ununiformed concrete surfaces in the field test.

*Keywords: Soil-structural interaction, Impact loading, Field test, Spread foundation, Friction*

## 1. INTRODUCTIONS

It has been observed during recent severe earthquakes in Japan that damage of existing reinforced concrete building structures were relatively minor compared to those estimated from the strong earthquake motions recorded on the ground surface, which often exceeded the current design standard level of Japan. The maximum inter-story drift on the time-history analysis using near-field ground accelerograms generally overestimates the observed damages, especially for the case of low-rise RC buildings. The reasons for this discrepancy may be estimated as: (1) the actual strength of the existing buildings might be generally higher than assumed in the analysis, (2) the story drift level estimated from residual crack widths might not correspond to the actual drift maximum responses and, (3) the earthquake intensities input to the buildings might generally be smaller than the motions recorded in the free fields, due to the soil-structure interaction or input loss at the foundation.

The effects of the soil structural-interaction might be identified through earthquake observation on the building and site by comparing accelerograms at the two sites, one on the ground surface and the other at the base foundation. The observed results would include the SSI effect from elastic theory as well as the non-linear deformation around the base foundation. However, it is still difficult to quantify the non-linear properties of the neighborhood soil, so that the lateral stiffness of the spread foundation is generally idealized to be elastic even in case of detailed soil-structure interaction analysis in Japan. The non-linear deformation around the base foundation would affect the inter-story drift response much more than the SSI analysis with elastic soil, especially in the case of a major earthquake and relatively higher shear strength around the footing area, such as low-rise building structures with spread foundations.

To identify the lateral stiffness of the spread base foundation including the non-linear deformation properties of the soil underneath, dynamic and static loading tests on an existing low-rise building were planned in this study. The impact and static lateral loads were applied at the level of the spread foundation in the existing three-story reinforced concrete school building in Ojiya City, Niigata

prefecture. The building was more than 45 years old and was subjected to major earthquake motion during the Niigata-ken Chuetsu earthquake 2004. However, the observed damages were minor, although a very strong motion up to 0.8g was recorded at the K-net Ojiya station, which was adjacent to the building site. Also it has been identified by aftershock observation (Kabeyasawa et al, 2006) that the intensities of the recorded motions were apparently different between the K-net station and the temporary station at the building base.

## 2. SCHOOL BUILDING FOR TEST

The floor plan and elevation of the tested part are shown in Fig. 1. and Fig. 2.

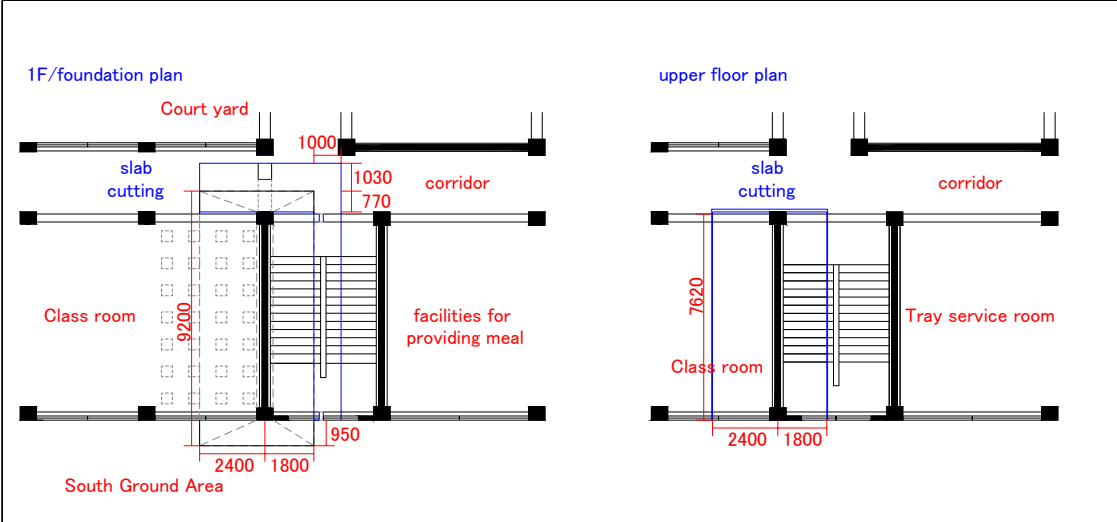


Figure 1. Floor plan of the tested part

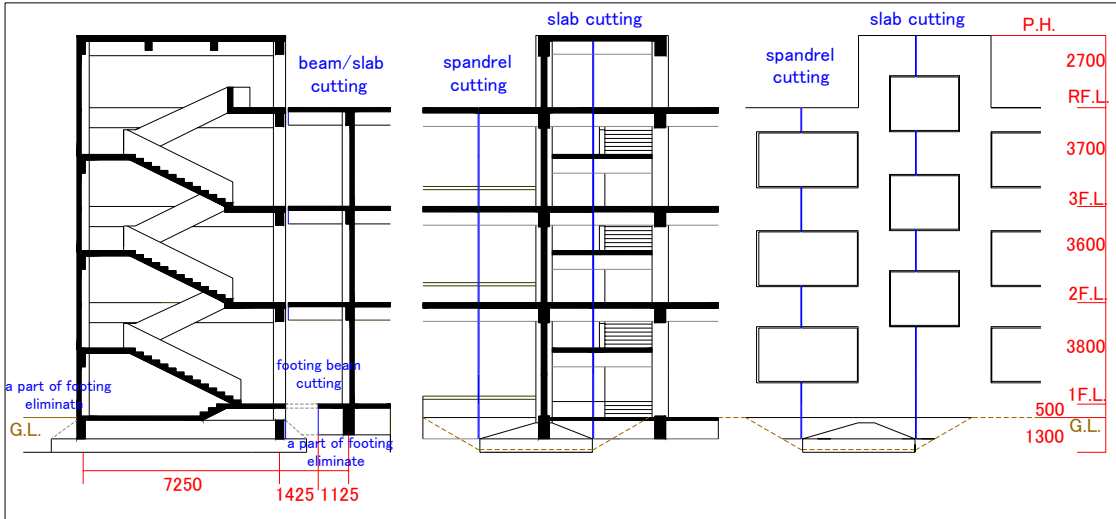


Figure 2. Elevation and section of the tested part

The school building is a three-story reinforced concrete structure with spread foundation constructed during 1960-1964. The loading test was carried out on a part of the structure in the southeast, which has one span each in longitudinal and transverse direction including structural a wall, stairs and a penthouse. The tested part was separated from the remaining mainframe through the base to the roof, cutting the footing/girder beams, slabs, and spandrels in each floor. The neighborhood soil around a footing of the specimen was removed up to the depth of the footing, except for the east side. The span

length is 4.2 m in the longitudinal direction, and 7.2 m in the transverse direction of the building, which was the loading direction. The story height is 4.25 m in the first floor, 3.6 m in the second floor, 3.7 m in the third floor, and 2.7 m as a penthouse. The first floor level in south area is 0.45 m lower than that in north area. The base foundation of the specimen has very large area under structural walls with the width of 4.2 m and the length of 9.2 m, and the height of the footing is 1.3 m. The estimated total mass of the tested part including the penthouse and the base foundation was 2215 kN.

### 3. PAST SURVEY ON GROUND

The fundamental period and the soil types of the ground in the area of the school building have been identified through the site investigation by the Building Research Institute (Okawa, 2006). The lateral loading test was carried out near the building. The result of the ground boring survey is shown in Table 1. The N-value for the standard penetration test was 1 above 1.30 m depth, and was very high (90+) under 1.30 m. The bottom of the building base foundation was 1.30 m depth from the ground level, which was landed on the stiff gravel underneath. The horizontal vs. vertical (H/V) spectrum obtained from micro tremor measurements is shown in Fig. 3. The fundamental period of the field ground was 0.12 s at the investigation site. The measured period was much lower than that at near field seismological station site (K-net Ojiya) by NIED, which was 0.28 (s).

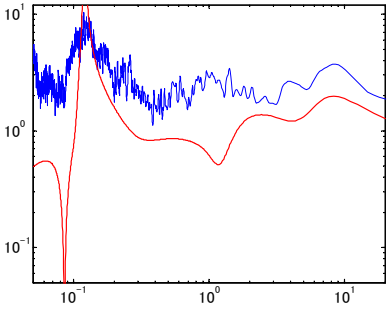


Figure 3. H/V Spectrum (Okawa, 2006)

Table 1. Soil type of the

Depth (m)	Type	Age	N
~ 0.50	Fill soil	Surface	1
~ 0.80	Clay	Surface	1
~ 1.30	Slit	Alluvial	1
~ 1.75	Fine sand	Alluvial	90+
~ 2.35	Gravel	Diluvia	90+

### 4. TEST PROCEDURE

#### 4.1. Impact loading test

The impact load was applied to the base foundation in the test, in such a way that the steel mass pendulum hanged from the roof of the main school building. The point of loading at the foundation beam was 0.55 m lower from the ground level. The loading system was shown in Fig. 4. and Fig. 5.



Figure 4. Rubber and Steel mass for impact loading

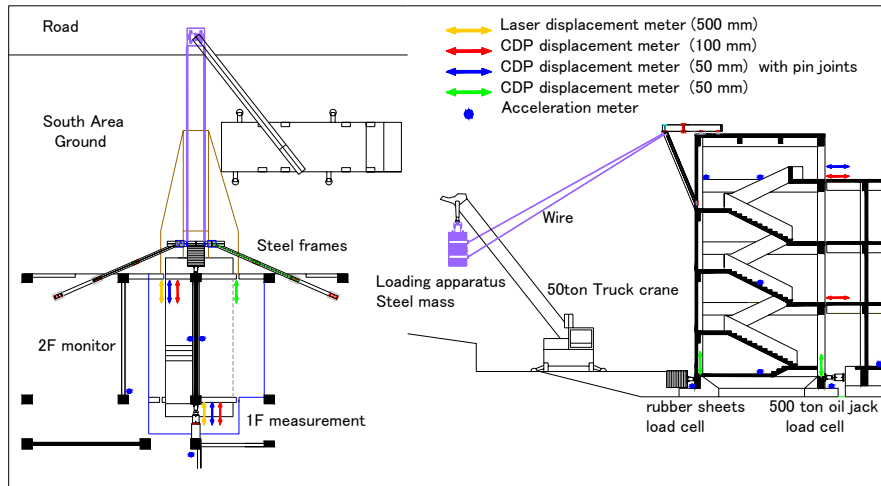


**Figure 5.** The system for impact and static loading

The steel frame was fixed on the roof and the beams of the remaining mainframe with post-tensioning PC bars, to suspend the steel mass and so as not to apply the reaction force to the tested part. The steel mass was suspended from the overhead steel frame on four points with wires and pin connections. The steel mass was lifted up to the target heights with a truck crane by wires connected to the loading apparatus attached to the mass. The steel mass consisted of 50 steel plates, each of  $1\text{ m} \times 1\text{ m} \times 0.04\text{ m}$ , and the total mass was up to 0.17 MN. A small oil jack in the loading apparatus was used to press and fix the wedge at the end of the mass, which could start the uplifted mass to drop off when the oil pressure was released.

The duration of impact loading would be too short, compared with the expected response period of the base foundation and the structure during earthquake, if the structural mass directly bumped on the base foundation. In order to make this duration as expected as in the earthquake response, absorbing rubber sheet was arranged at the side surface of the footing. The size of a sheet was  $1 \times 1 \times 0.1\text{ m}$ . The total thickness (1.2 m) or the number of rubbers (initially twelve) was selected based on the duration estimated from the potential energy and the stiffness of rubbers so that the duration would be equal to 0.05 seconds, which is one-quarter of the structural period (5 Hz). A load cell was installed between the steel plate at the end of the rubbers and the footing to measure the impact load. The relative displacements to the mainframe and the absolute accelerations were measured at each floor level.

#### 4.2. Static loading test

The static loading test was also carried out during impact loading tests from the other side of the school building. An oil jack and load cell of 5 MN capacity was set at the foundation level between the tested part and the remained mainframe for reaction as shown in Fig. 6.



**Figure 6.** Static loading system

The transverse foundation beam in north section was cut and the middle part of 1.2 m length was removed for static loading. The lateral shear force by the oil jack at the level of the foundation beam expanded the two parts in the sliding mechanism. The loading level was same as that of the impact loading. The static lateral loading and unloading were done in one direction. The target loading force is selected, which would not exceed the previous impact loading level. The displacement of the tested part was measured also with the gauge located at each floor level

## 5. TEST RESULT

### 5.1. Measured displacement and shear force

It took three weeks for setup of the equipment of these tests, such as cutting concrete, setting steel frame, oil jack, and measurement. The loading test was done from 22 to 25 of April 2010, after the school moved to a new building and during demolish of the old building. The maximum displacement, shear force, and foundation base shear coefficient from the test are listed in Table 2. The displacements were those measured in the opposite side from the loading side, which did not include the axial compression strain of the base foundation. The maximum shear forces were evaluated as the shear resistance beneath the bottom of the base foundation, which were derived as sum of the impact load from the steel mass measured by the load cell and the inertia forces calculated from the accelerations measured in each floor level.

The first test of impact loading was conducted on 10:00am, April 22, 2010. The steel mass was dropped off from the height of 1.5 m. The number of rubber sheets was set as twelve. The first test of static loading was carried out on 12:00 after the impact loading. The second test of impact loading was carried out on 1:00pm of the same day by dropping off the mass from the height of 6.0 m. However, the suspending wires ( $\phi=30$  mm) broke, because of unexpected higher rotational inertia forces of the mass. The corner of the steel mass landed in a moment though bumped to the center of the footing. The third test of impact loading was carried out on 10:00am, April 24 after the replacement with the wires of  $\phi=40$  mm. The loading height was 7.5 m. The second test of static loading was carried out after the test. The number of the rubber sheet decreased to eight on the final impact-lading test in order to shorten a period of the external load. The mass height was also 7.5 m. On 10:00, 25 April, the pushover static loading was carried out to investigate the static lateral resistance or the friction coefficient of the base at large displacement level.

Relative displacements to the mainframe were measured at 24 points including relative lateral deformations at the foundation beam, the second to the roof floor in the loading directions. The lateral accelerations were also measured in each floor. Relative vertical deformation also measured at 4 points to estimate the rocking deformation as well. The displacements and accelerations were recorded during the impact loading tests with the time interval of 0.004 seconds.

**Table 2.** Test results

	The maximum response on impact loading			The maximum response on static loading			
	Displacement (mm)	Loads (kN)	Base shear coefficient		Displacement (mm)	Loads (kN)	Base shear coefficient
No.1	0.69	1794	0.81	No.1	0.56	1132	0.51
No.2*	1.28	2045	0.92	No.2	2.86	3430	1.55
No.3	1.79	3299	1.49	No.3	300	4645	2.10
No.4	5.78	4931	2.23	After base slip		3180	1.44

\* Loading force reduced because suspending wires broke and corner of the steel mass landed

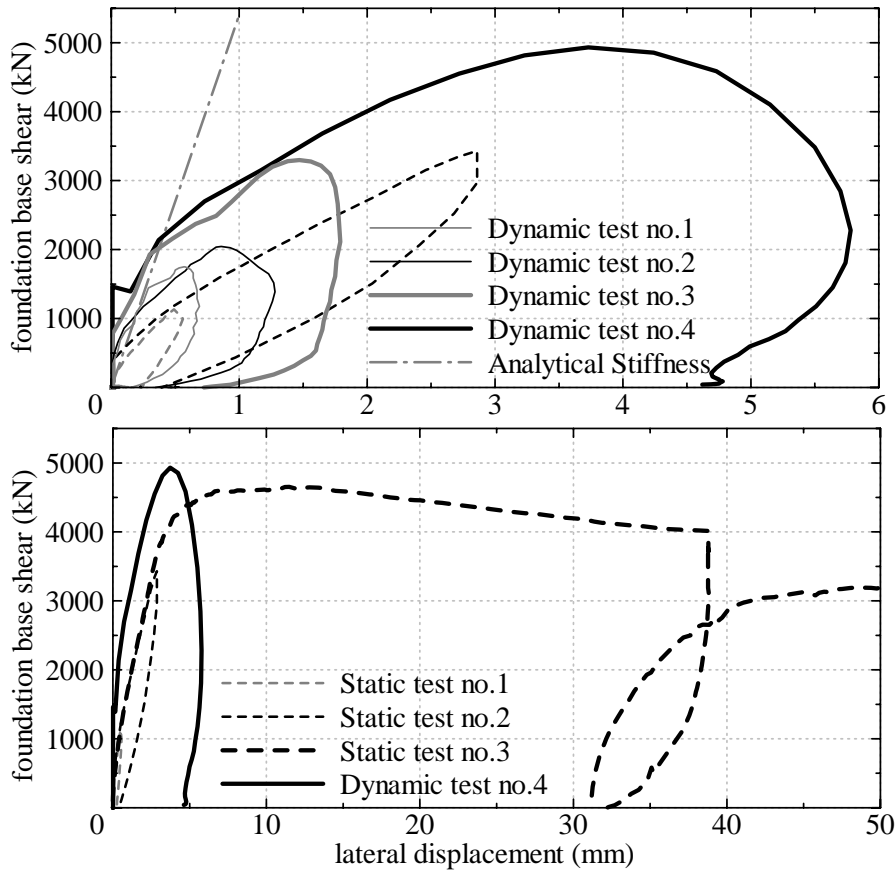


**Figure 7.** The relationships between the lateral force and the displacement of the foundation

The maximum shear resistance of the footing was 1794 kN at the lateral displacement of 0.69 mm from the first test of impact loading. The base shear coefficient was 0.81 based on the estimated total mass of 2215 kN. On the other hand, the maximum static force was much lower 1132 kN at the nearly same displacement level of 0.56 mm. The maximum base shear coefficients recorded in the second and third tests of impact loading were 1.49 and 2.23, respectively, which were relatively higher as general friction coefficients at the discontinuous face.

The relationships between the base shear and the displacement are shown in Fig. 7. The non-linear behavior was observed as a hysteretic shape on the impact and static tests, while the maximum response displacements by the impact loading might not be large enough such as 5.78 mm during the 4<sup>th</sup> dynamic test. The maximum shear coefficient attained up to 2.10 during the pushover static loading test, which gradually decreased to around 1.44 under larger displacement, probably falling down to the friction coefficient of sliding.

## 5.2. Stiffness and period from the impact and static loading tests

The secant stiffness to the maximum displacement and the elastic stiffness, which are defined at the displacement of 0.15 mm are shown in Table 3. The periods of the impact loads are also shown in the table, which are estimated from the time duration until the maximum response as one-quarter of one cyclic response. The secant stiffness gradually decreased while the maximum load attained large peak values in the impact and static loading tests. However, the elastic stiffness increased with the maximum displacement in the impact loading tests while it was almost constant though the three static loading tests. It might be explained by creep deformation of the ground soil influenced the stiffness in the static loading. Although the period of the impact loads decreased in the final test due to the reduced number of the rubber sheets, the period in the impact loading tests approximates generally to the target as the estimated fundamental period of the structure (5~6 Hz).

**Table 3.** Stiffness and period on the impact-loading test

Impact loading	Secant Stiffness (kN/mm)	Elastic Stiffness (kN/mm)	Stiffness ratio to 1 <sup>st</sup> test result	Stiffness ratio to Elastic stiffness	Period (s)
No.1	3147	5260	1.000	0.598	0.256
No.2	2378	6250	0.756	0.380	0.256
No.3	2244	7650	0.713	0.293	0.208
No.4	1321	9480	0.419	0.139	0.160
Static loading	Secant Stiffness (kN/mm)	Elastic Stiffness (kN/mm)	Stiffness ratio to 1 <sup>st</sup> test result	Stiffness ratio to Elastic stiffness	
No.1	2311	3399	1.000	0.680	
No.2	1199	3565	0.519	0.336	
No.3	726	3489	0.314	0.208	

The elastic stiffness of the spread foundation in the lateral direction was evaluated from a theoretical Eqn. 5.1. The shear velocity  $V_s$  for the gravel under the footing was investigated from an empirical Eqn. 5.2. (AIJ, 1987), based on soil types and N-value. The theoretical stiffness  $K_0$  was 5400 kN/m, which approximated an elastic stiffness of 5260 kN/m from 1<sup>st</sup> impact loading test.

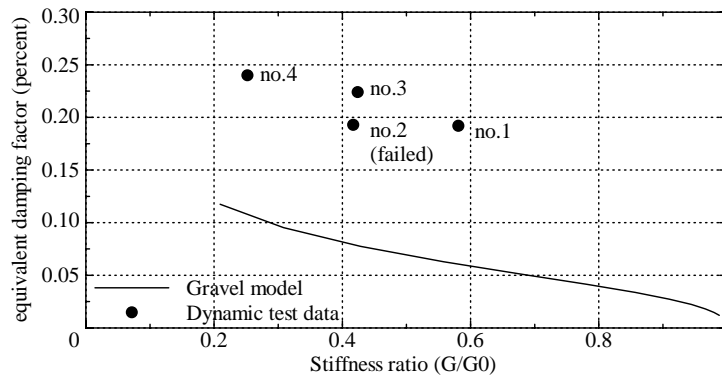
In guidelines for Japanese capacity spectrum design, a design procedure for reinforced concrete structure considering soil-structural interaction is introduced. In this procedure, the equivalent damping coefficient for interaction spring model was derived only from the hysteretic damping of soil material, when a period of the ground was smaller than that of the upper structure (BCJ, 2001). The equivalent viscous damping factor  $h_{eq}$  for the soil materials were investigated from a ratio of the secant stiffness to the theoretical elastic stiffness, and compared with the test results from the impact loading. The relation between shear stiffness  $G$  and shear strain  $\gamma$ , and the relation between damping coefficient  $h_{eq}$  and shear strain  $\gamma$  are evaluated based on Imatsu-Fukutake model (1986) as shown in Eqn. 5.3. The impact-loading test result only shows hysteretic shape for loading and unloading in one direction. The equivalent damping coefficient was evaluated simply with twice of the hysteretic energy dissipation in load-displacement relationship so as not to overestimate them. The damping coefficients estimated between the equation and test results are compared in Fig. 8. The equivalent damping coefficients in the tests of impact loading are much larger than estimated from the standard model for gravel. The reasons for this discrepancy might be due to an effect of friction on the side surface or broken stones under the base foundation, which should be investigated further.

$$K_0 = 8GR / (2 - \nu) \quad (kN / m) \quad R = 3.13 (m) \quad K_0 = 5400 (kN / m) \quad (5.1)$$

$$V_s = 136 N^{0.246} \quad (m / s), \quad G_0 = \rho V_s^2 \quad (kN / m^2) \quad (5.2)$$

$$G / G_0 = 1 / (1 + 12.4 \gamma^{0.75}), \quad h_{eq} = 18.9 \gamma^{0.30} \quad (5.3)$$

where,  $\gamma$ : shear strain (%),  $\rho$ : specific weight for soil (=1.8 (kN/m<sup>3</sup>)), R: a radius of an aerial equivalent circular foundation (m),  $\nu$ : Poisson's ratio(=0.30)

**Figure.8.** Comparison of the equivalent damping coefficients  $h_{eq}$  from the test and gravel model

## 6. STATIC LOADING TEST FOR CONCRETE FRICTION COEFFICIENT

### 6.1. Outline of static loading test

In above study on the field site loading test, the lateral strength of base foundation seems to increase for bonding or interlocking on ununiformed concrete surfaces from simple friction. Another static cyclic loading test was carried out in order to evaluate general friction coefficient on flat concrete surface.

The specimen consists of two parts as shown in Fig. 9. A footing concrete was placing on the levelling concrete as a conventional spread foundation in Japan. The contact area of the sliding surface is  $800 \times 500$  mm assuming the minimum size for the independent footing dimension. The concrete contact surface was smoothed with trowel. The compressive strengths of concretes were  $33.5 \text{ (N/mm}^2\text{)}$  for base foundation and  $26.2 \text{ (N/mm}^2\text{)}$  for levelling concrete in the material test.



**Figure 9.** The lateral loading test of the placing concrete joint in the laboratory

Twice cyclic loading was carried out within  $\pm 10$ mm footing drift for each axial loads. Generally, bending moment occurs at the bottom of the base foundation during earthquake, because the inflection point is higher than a concrete contact surface. In this test, the contribution of bending moment to reduce the friction force was ignored in order to evaluate the friction coefficient without such a variable factor in time history response. The axial stress on the specimen varied during cyclic loadings, which is equivalent to the practical allowable stress for sustained loading on base foundation (fine sand, clay and gravels) in the building design

### 6.2. Result of static loading test

The load displacement relation in the loading test is shown in Fig. 10. Slipping drift represents an average value in central axis of the specimen. The loading force was scaled into a friction coefficient, which was divided by a summation of input vertical force and self-weight (18 kN). The maximum, minimum, and average friction coefficients of concrete were shown in Table 4. The maximum coefficient was 1.046, while the average was 0.754 during the loading test. The maximum coefficient are recorded without vertical load, which was not influenced by bonding strength of concretes

The base shear coefficient at the beginning of the slip behaviour is around 0.8 in each loading cycle, especially shows large value in a cycle axial load decreased (360 to 30 kN, 180 to 0 kN), and gradually saturates during steady slip behaviour. The stick-slip behaviour was observed when axial stress on the specimen exceeded  $240 \text{ kN/m}^2$ , and the distinction between the maximum and minimum coefficient is in proportional to the axial loads.

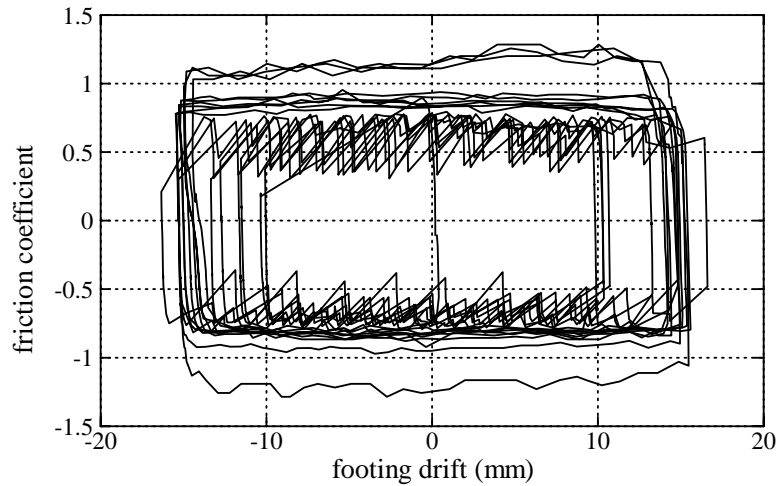
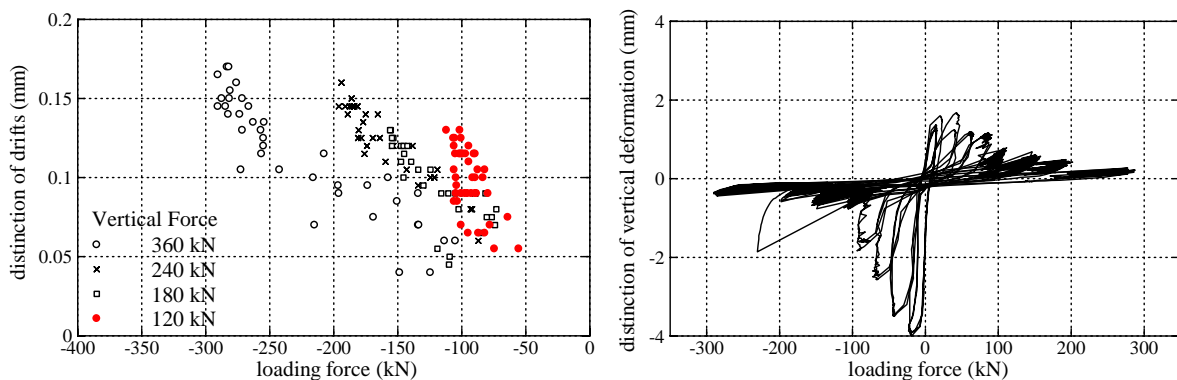


**Figure.10.** Load displacement relation of the placing concrete joint

**Table 4.** Test results

Vertical load (kN)	Shear coefficient (Positive)		Shear coefficient (Positive)	
	Maximum	Average	Maximum	Average
240	0.771	0.641	0.767	0.619
120	0.792	0.713	0.786	0.678
360	0.763	0.613	0.769	0.603
30	0.925	0.876	0.934	0.896
60	0.848	0.812	0.924	0.842
90	0.844	0.792	0.862	0.812
180	0.814	0.639	0.779	0.596
0	1.103	0.978	1.271	1.108

Fig. 11 (a) shows a relation between loading force and distinction of measured displacement on both edges. The shrink deformation of footing concrete related with the sudden reduction of the friction force as shown in the figure. This sudden slip behaviour occurs with releasing compressive strain energy for the ununiformed shear stress on the contact surface. Fig. 11 (b) shows a relation between loading force and distinction of vertical displacements on both edges. Distinction of vertical deformation was obvious when loading force was smaller. The contact area for shear friction leans in slipping direction, and vertical deformation concentrated in one side in these cases. These tests indicate the friction force between concrete surfaces increases by localization of shear or axial contribution.



(a) loading force and distinction of drifts      (b) loading force and distinction of vertical deformation

**Figure 11.** Relation between loading force and shear contribution on contact surface

## 7. CONCLUDING REMARKS

The impact and static loading tests were carried out on the base foundation of an existing reinforced concrete structure. The methods and results of the tests are reported in this paper. The lateral stiffness and equivalent damping coefficient are compared with theoretical calculation. The elastic stiffness from the test of impact loading approximated to the theoretical stiffness. The secant stiffness to the maximum loads gradually decreased with non-linear maximum response of the ground soil, though the inelastic displacement was not large enough in the test of impact loading. The equivalent damping coefficients from the tests were much higher than the theoretical estimate, the reason for which should be investigated further. The friction coefficient on concrete surfaces was usually around 0.8, but that value increases by localization of shear or axial stress on surface, which was verified in static friction test in the laboratory.

## ACKNOWLEDGEMENT

The site experiment reported in this paper was supported by the Grants in Aid for Scientific Research from JSPS (Grant no. 21760428 and 19360246) and the Grant for Research by the Gunma-ken Structural Engineering Center. The Education Board of the Ojiya City provided us with a chance to execute the experiment on the old school building to be demolished at time of the replacement with the new one. The efforts in operating the test set-up by the Asiss Corporation, the Maruyama Construction Company, and Members of Kabeyasawa laboratory, ERI, are gratefully acknowledged.

## REFERENCES

- Kabeyasawa, T. Kabeyasawa, T. Sakaue, M. Tanaka, Y. and Namegaya, Y. (2006). Identification of input loss in base motion on observation of aftershocks and damages to buildings after Niigata-Chuetsu earthquake, *Journal of Structural Engineering*. **Vol.52B**
- Kabeyasawa, T. Kabeyasawa, T. Kouketsu, K. Kudou, K. and Sanada, Y. (2006). Identification of input loss in base motion based on observation of aftershocks at Ojiya elementary school after Niigata-ken Chuetsu earthquake. *AIJ annual conference report*. **C-2: 453-454**
- Okawa, I. et al. (2006). Ground survey around Ojiya elementary school. *BRI annual report*. **Vol.42**.
- Architectural Institute of Japan, (1987). Introduction to soil-structural interaction theory.
- The Building Center of Japan, (2001). Capacity spectrum design and examples 2001.
- Imatsu, M. & Fukutake, T. (1986). Dynamic response property for gravel material, *21st soil engineering research conference: 509-512*